ARTICLE

Immunohistochemical characterisation of the immune landscape in primary uveal melanoma and liver metastases

Pascale Mariani[1], Nouritza Torossian[2], Steven van Laere[3], Peter Vermeulen[3], Leanne de Koning[4], Sergio Roman-Roman[4], Olivier Lantz[5,6,7], Manuel Rodrigues[2,8], Marc-Henri Stern[8], Sophie Gardrat[9], Laetitia Lesage[9], Gabriel Champenois[9], André Nicolas[9], Alexandre Matet[10,11], Nathalie Cassoux[10,11], Vincent Servois[12], Emanuela Romano[2], Sophie Piperno-Neumann[2], Claire Lugassy[4] and Raymond Barnhill[4,11]✉

BACKGROUND: The immune landscape of uveal melanoma liver metastases (UMLM) has not been sufficiently studied.
METHODS: Immune cell infiltrates (ICIs), PD-1 and PD-L1 were characterised in 62 UMLM and 28 primary uveal melanomas (PUM). ICI, PD-1 and PD-L1 were scored as: (1) % tumoral area occupied by tumour-infiltrating lymphocytes or macrophages (TILs, TIMs) and (2) % perTumoral (perT) area. ICIs and other variables including histopathologic growth patterns (HGPs), replacement and desmoplastic, of UMLM were analysed for their prognostic value.
RESULTS: ICIs recognised by haematoxylin-eosin-saffron (HES) and IHC (e.g., T cells (CD3), B cells (CD20). Macrophages (CD68), (CD163), were primarily localised to the perT region in PUM and UMLM and were more conspicuous in UMLM. HES, CD3, CD4, FoxP3, CD8, CD20, PD-1 TILs were scant (<5%). TIMs were more frequent, particularly in UMLM than in PUM. Both CD68+ TIMs and HGPs remained significant on multivariate analysis, influencing overall (OS) and metastasis-specific overall survival (MSOS). CD68 +, CD163+ and CD20+ perT infiltrates in UMLM predicted increased OS and MSOS on univariate analysis.
CONCLUSIONS: TILs and PD-L1 have no predictive value in PUM or UMLM. CD68+ and CD163+TIMs, CD20+ perT lymphocytes, and HGPs are important prognostic factors in UMLMs.

British Journal of Cancer (2023) 129:772–781; https://doi.org/10.1038/s41416-023-02331-w

INTRODUCTION

Uveal melanoma (UM) is the most common primary cancer of the eye [1–4]. It is nevertheless a relatively rare disease, occurring with an incidence of ~5 per million and representing about 5% of all melanomas. Nearly half of the patients will develop metastases, affecting the liver in more than 90% of cases. Once patients develop metastatic UM, the prognosis is poor with a median survival of ~12 months [1–4]. Genetic alterations (monosomy 3 and gain in chromosome 8q), observed in primary uveal melanoma (PUM), are predictive of an increased risk of developing metastases [5, 6], but have no prognostic value once liver metastases have developed [7, 8].

Although immune checkpoint inhibitors are frequently administered for UMLM, response rates to these agents are low, i.e., ~5% [9]. However, exceptional responses to these therapies have recently been reported, suggesting that some patients may benefit from immune checkpoint inhibitors [9–13]. Recently, the bispecific fusion protein Tebentafusp, which redirects T cells towards melanoma cells expressing gp100, has been shown to improve outcome in patients with UMLM [14, 15]. Given these encouraging results, it is important to characterise the immune cell infiltrates of UMLM and to understand how these infiltrates contribute to immunotherapy response or resistance as well as patient outcome.

While the presence of tumour-infiltrating T cells (TILs) is associated with a good prognosis in a wide variety of cancers, including skin melanoma, breast, colorectal and prostate cancer, T-cell infiltration in PUM has been reported to connote an adverse prognosis [16–24]. Infiltration of PUM by macrophages, especially the pro-tumorigenic M2 phenotype, is suggested to be associated with monosomy 3 and poor prognosis [18, 25–29]. However, the immune cell infiltrates (ICI) in liver UMLM are poorly described, mostly because UMLM are not easily accessible for extensive biopsy sampling [7].

We have recently reported for the first time the presence of particular "histopathological growth patterns" (HGPs), "replacement" and "desmoplastic", in both uveal and cutaneous melanoma liver metastases [7, 30]. These HGPs have been previously described in liver metastases from colorectal, breast, and pancreatic carcinomas [31]. The replacement HGP is defined by tumour cells that progressively infiltrate and replace hepatocytes at the perTumoral–stromal interface, i.e., the advancing front of

[1]Department of Surgery, Institut Curie, Paris, France. [2]Department of Medical Oncology, Institut Curie, Paris, France. [3]Faculty of Medicine and Health Sciences, University of Antwerp–MIPRO Center for Oncological Research (CORE) - TCRU, GZA Sint-Augustinus, Antwerp, Belgium. [4]Department of Translational Research, Institut Curie, Paris, France. [5]Laboratoire d'immunologie clinique, Institut Curie, Paris, France. [6]Centre d'investigation Clinique en Biothérapie, Institut Curie (CIC-BT1428), Paris, France. [7]INSERM U932, PSL University, Institut Curie, Paris, France. [8]Inserm U830, DNA Repair and Uveal Melanoma (D.R.U.M.), Equipe Labellisée Par la Ligue Nationale Contre le Cancer, Institut Curie, Paris, France. [9]Department of Pathology, Institut Curie, Paris, France. [10]Department of Ophthalmology, Institut Curie, Paris, France. [11]Université de Paris Cité UFR de Médecine, Paris, France. [12]Department of Radiology, Institut Curie, Paris, France. ✉email: raymond.barnhill@curie.fr

Received: 8 February 2023 Revised: 16 May 2023 Accepted: 16 June 2023
Published online: 13 July 2023

the metastasis. In contrast, the desmoplastic HGP is defined by a distinct separation of the metastasis from the liver parenchyma by a peripheral annulus (band) of desmoplastic fibrous tissue. In examining 41 UM liver metastases in 41 patients, we found that the replacement HGP involves ~75% of resected UMLMs and is associated with a strong adverse prognosis [7, 32], providing for the first time an important tissue biomarker for prognosis after the development of liver metastases in UM.

In this study, we have characterised the ICIs and PD-1 and PD-L1 status by immunohistochemistry in a series of resected liver metastases in comparison with PUMs. We relate our results to HGPs and various other clinical, histopathological, and genetic prognostic factors.

MATERIALS AND METHODS

Study population

A retrospective study of primary uveal melanoma and corresponding hepatic metastases from the period 2006 to 2017 was conducted. 28 PUM and 62 UM liver metastases were retrieved from the archives of the Pathology Service, Institut Curie (IC). The 62 UMLM have been previously utilised in a comprehensive study of HGPs [8]. Among these were 21 matched PUM and UMLM samples from 21 patients. This study was approved by our institutional ethics committee. Written informed consent for the use of tissues and data for research was signed by each patient. The study complied with the principles of the Declaration of Helsinki.

Patient information

Clinical, histopathologic, molecular genetic, and long-term follow-up information for these patients has been collected prospectively as previously described [7, 33]. The following patient characteristics were analysed: age (years); gender; genetic analysis (see below) and BAP1 status; local therapy of the primary melanoma (proton beam therapy, radioactive (iodine) disc brachytherapy, enucleation); treatment of liver metastases (1: surgery alone initially, 2: systemic alone, 3: best supportive care (BSC, palliative)); R (resection) status of metastasis: R0—resection complete, R1—microscopically incomplete, R2—macroscopically incomplete; disease-free interval (time to metastasis); overall survival (OS) and liver metastasis-specific overall survival (MSOS).

Histopathological examination

Formalin-fixed, paraffin-embedded (FFPE) 5-µm sections were prepared for each enucleation and liver metastasis for microscopic examination. Whole glass slides were digitised with a Phillips pathology slide scanner (Phillips Healthcare, Amsterdam, the Netherlands). Criteria for the selection of metastases were as follows: if more than one metastasis was present, criteria for selection included metastases having a 360-degree circumference surrounded by viable intact liver parenchyma, or those with the highest percentage of the peripheral circumference (of the metastasis) surrounded by liver parenchyma, and absence of significant necrosis, scarring, or disruption of either the metastasis or the liver.

Histopathological characteristics recorded for each enucleation were as follows: maximum UMLM tumour diameter (in mm), principal melanoma cell type (Histotype) (modified Callender classification [34, 35]: epithelioid, spindle, or mixed); local extension of the primary tumour (ciliary body, optic nerve or extraocular extension); melanin content: percentage of tumour containing melanin, intensity of cytoplasmic melanin (0—absent, 1—faint -1, 2—moderate, 3—high, 4—very high), and melanin index (percentage melanin x intensity = index (0 to 400)).

Histopathologic characteristics recorded for each liver metastasis in Table 2. and based on the examination of 1 representative hematoxylin, eosin and saffron-stained section or digital image for each case included: the histopathologic growth pattern of the liver metastases (HGP); the HGP was scored according to consensus guidelines as described by Latacz et al. [36]. Metastases of all sizes were included and there was no bias toward the selection of small metastases. The liver metastasis HGP assessment consisted of the percentage of the circumference involved (at least 5%) by desmoplastic, replacement or pushing HGP. The predominant HGP (≥50% of the circumference) was used for all analyses; melanin content: percentage of tumour containing melanin, intensity of cytoplasmic melanin (0—absent, 1—faint -1, 2—moderate, 3—high, 4—very high), and melanin index (percentage melanin × intensity = index (0–400)) [37, 38].

The images were reviewed independently by two experienced senior pathologists (RB and PV) without specific knowledge of the case or clinical outcome.

Genetic analysis

In total, 91 specimens had sufficient tumour from frozen tissue samples for array comparative genomic hybridisation (aCGH), as previously described [6]. Both primary and metastatic samples were utilised if tissue was available. Two patients had no primary or metastatic tumour available. In brief, 91 tumour samples from 20 enucleations, 9 fine-needle aspirations and 62 resected liver metastases, including 6 cases with material from both primary tumours and liver metastasis, were studied. Among the 14 frozen samples from the liver, 2 were excluded because of inadequate aCGH results. Only the status of chromosomes 3 and 8 (8q) was assessed.

The risk for the development of metastasis in patients with four genomic profiles was analysed. These four risk groups [6] were defined by the presence or absence of chromosome 3 loss (monosomy 3) and the presence or absence of chromosome 8 gain (including gain of the entire 8 chromosomes, gain of the entire 8q, and distal gain of 8q), as follows: Group 1, Low risk for metastasis: normal status of chromosomes 3 (disomy 3) and 8 (8 nl): D3/8 nl; Group 2, Intermediate risk: monosomy 3 and normal status of 8: M3/8 nl; Group 3, Intermediate risk: disomy 3 and gain of 8q (8 g): D3/8 g; and Group 4, High risk: M3/8 g (Tables 1 and 2) [6]. For this analysis, the aCGH strata were compiled by combining data from primary and metastatic samples, to circumvent the high numbers of missing data in both individual series.

Immunohistochemistry

IHC was performed on a single FFPE section corresponding to the representative HES section (4-µm thickness) for each immunomarker, as follows: CD3 (Dako, A0452, 1/200), CD4 (Dako, 4B12, IR649, undiluted), FOXP3 (Abcam, ab20034, 1/200), CD8 (Dako C8/144B, IS623, undiluted), CD20 (Dako, L26, IR602, 1/200), CD68 (Dako, KPI, M0814 1/800), CD163 (Novocastra, NCLCD163, 1/200), PD-1 (Bio SB, BSB6217, 1/50), PD-L1 (Dako, 22C3, dilution 1/50), and BAP1 (Santa-Cruz, sc-28383, 1/50). PD-L1 immunostaining using Dako clone 22C3 was performed on 20 liver metastases by the Merck Research Laboratory (Palo Alto, CA, USA) using chromogens DAB or Vector Red and Vina Green in case of heavy melanin content in tumoral tissue.

Immune cell infiltrates and immune checkpoints were semi-quantitatively scored by pathologists RB (100% of specimens) and SG (~25% of specimens) with concordance, using the method of Rothermel [39], which was modified to include: (1) the entire tumoral area occupied by tumour-infiltrating lymphocytes (TILs) in % area of tumour and (2) the % of the entire circumferential area occupied by peri-tumoral immune cell infiltrates (PerT) identified in Hematoxylin, Eosin, Saffron (HES)-stained sections and in immunohistochemical-stained sections with the antibodies described above. This circumferential area (interface or advancing front) is a circumferential annulus of variable thickness ranging from ~1 to 4 mm and including a peripheral rim of tumour cells, a desmoplastic rim (if present), and surrounding hepatocytes. HES-stained sections were used to score the total number of lymphocytes present.

Scoring was:
0 = absent;
1 = rare, <5% of tumoral or peri-tumoral areas positive;
2 = > 5–50% of tumoral or peri-tumoral areas positive; and
3 = > 50–100% of tumoral or peri-tumoral areas positive.

Scoring of PD-L1 expression utilising Dako clone 22C3 was based on % of tumour cell expression (TC) and % of immune cells (IC) in the peri-tumoral stromal area, both in a typical membranous pattern. Scoring was then recorded as follows:
0 = absent
1 = < 10% stained cells
2 = > 10–50% stained cells
3 = > 50–100% stained cells.

Statistical analysis

Data were analysed using R statistical software (https://cran.r-project.org). Prior to data analysis, missing data were imputed using the k-nearest neighbour algorithm (impute package in R). Notably, samples with more than 75% missing data were filtered out prior to imputation and were left out of the analysis. Next, the relationships between HGP and other categorical variables on the one hand and the ordinal immune staining scores on the

Table 1. Distribution of clinicopathological variables in a series of 28 primary uveal melanomas.

Variable	Category	
Age	Mean (+/− SE)	54.0 (+/−2.3)
Gender	Female	$N = 17$
	Male	$N = 11$
Tumour diameter	Mean (+/− SE)	16.6 (+/− 0.5)
Histotype	Epithelioid	$N = 14$
	Spindle	$N = 4$
	Mixed	$N = 6$
	NA	$N = 4$
Local extension	Ciliary body	$N = 8$
	Optic nerve	$N = 0$
	Scleral extension*	$N = 2$
	None	$N = 18$
Melanin index	Mean (+/− SE)	149.1 (+/− 24.8)
HGP	Desmoplastic	$N = 5$
	Replacement	$N = 17$
	NA	$N = 6$
aCGH status	D3/8 g	$N = 4$
	M3/8 g	$N = 20$
	M3/8 N	$N = 4$
	D3/8 N	$N = 0$
BAP1 loss	No	$N = 8$
	Yes	$N = 17$
	NA	$N = 3$
Treatment	Enucleation	$N = 23$
	Proton	$N = 5$
	Brachy	$N = 0$
Overall survival (months)	Median (95%CI)	49.7 (34.7–NA)
Metastasis-specific overall survival	Median (95%CI)	26.2 (16.3–82.5)

*Angiotropism in sclera (2 cases), 1 case angiotropism and neurotropism.

other hand were evaluated using the Kruskal–Wallis test using the categorical variables as strata. For relationships with continuous clinicopathological variables (e.g., age, tumour diameter, melanin index), the Kruskal–Wallis test was also used but now using the immune staining scores as strata. The comparison of the primary and metastatic uveal melanoma samples was analysed both in paired and unpaired fashion with the Wilcoxon test. The survival analyses included overall survival (OS), and liver metastasis-specific overall survival (MSOS). Patients were censored when alive at last follow-up or when lost to follow-up. OS was defined as the difference between the time of diagnosis of the PUM and time of death or the last follow-up. MSOS was defined as the difference between time of diagnosis of the UM metastasis and time of death or last follow-up. Differences in survival were calculated using the log-rank test and visualised using Kaplan–Meier curves (survminer package in R). Univariate and multivariate hazard ratios (HR) were calculated using the Cox proportional hazards model. All statistical tests were considered significant with P value < 0.05. Variables that were not significant in univariate analysis were removed before the multivariate analysis was conducted.

RESULTS

Primary uveal melanomas

Clinical, histopathologic and genetic findings. Overall, 28 primary uveal melanomas (PUMs) were examined. The dataset including age, gender, tumour diameter, melanoma cell type (Histotype), local extension of the PUM, melanin index, the predominate (≥50% desmoplastic or replacement) histopathological growth pattern (HGP) of the liver metastases, aCGH risk groups, BAP1 loss status, treatment of the PUM (enucleation, proton, brachytherapy), median overall survival, and median metastasis-specific overall survival is provided in Table 1.

Table 2. Distribution of clinicopathological variables in a series of 62 uveal melanoma liver metastases.

Variable	Category	
Age	Mean (+/− SE)	53.5 (+/−1.5)
Gender	Female	$N = 31$
	Male	$N = 31$
HGP	Desmoplastic	$N = 15$
	Replacement	$N = 47$
Melanin index	Mean (+/− SE)	211.0 (+/− 21.4)
aCGH status	D3/8 g	$N = 18$
	D3/8 N	$N = 3$
	M3/8 g	$N = 34$
	M3/8 N	$N = 6$
	NA	$N = 1$
BAP1 loss	No	$N = 17$
	Yes	$N = 39$
	NA	$N = 6$
Resection margin	R0	$N = 37$
	R1	$N = 6$
	R2	$N = 14$
	NA	$N = 5$
Treatment	BSC	$N = 10$
	Surgery	$N = 33$
	Systemic	$N = 19$
Overall survival (months)	Median (95% CI)	61.4 (47.2–113.9)
Metastasis-specific overall survival (months)	Median (95% CI)	27.3 (19.5–45.2)

Uveal melanoma liver metastases

Clinical, histopathologic and genetic findings. In total, 62 resected uveal melanoma liver metastases were analysed (Table 2). The dataset including age, gender, histopathological growth patterns, melanin index, aCGH risk group, BAP1 loss status, margin status after resection (R0, R1, R2), and treatment (surgery alone, systemic therapy alone, best supportive care) is provided in Table 2.

Differences in some shared parameters in Tables 1 and 2, e.g., median overall survival, are explained by differences in the cohort sizes and compositions between the two groups.

The immune landscape: the scoring of immune cell infiltrates and immune checkpoints in PUM and UMLM by light microscopy and immunohistochemistry

The scoring of the immune cell infiltrates, i.e., lymphocytes and macrophages, was compared in both paired PUM-UMLM ($n = 21$) and total PUM-UMLM (PUM $n = 28$ and UMLM $n = 62$), utilising the Wilcoxon test. Significant differences between PUM and UMLM are presented in boxplots for the paired analysis (Fig. 1) and the total analysis (Fig. 2) and summarised in Supplemental Table 1. These infiltrates, which were recognised by light microscopy (HES stain) and immunohistochemistry, were primarily localised to the peritumoral stromal region in both primary tumours and metastases (HES, CD3, CD68, CD163) (Figs. 3 and 4) and were more conspicuous

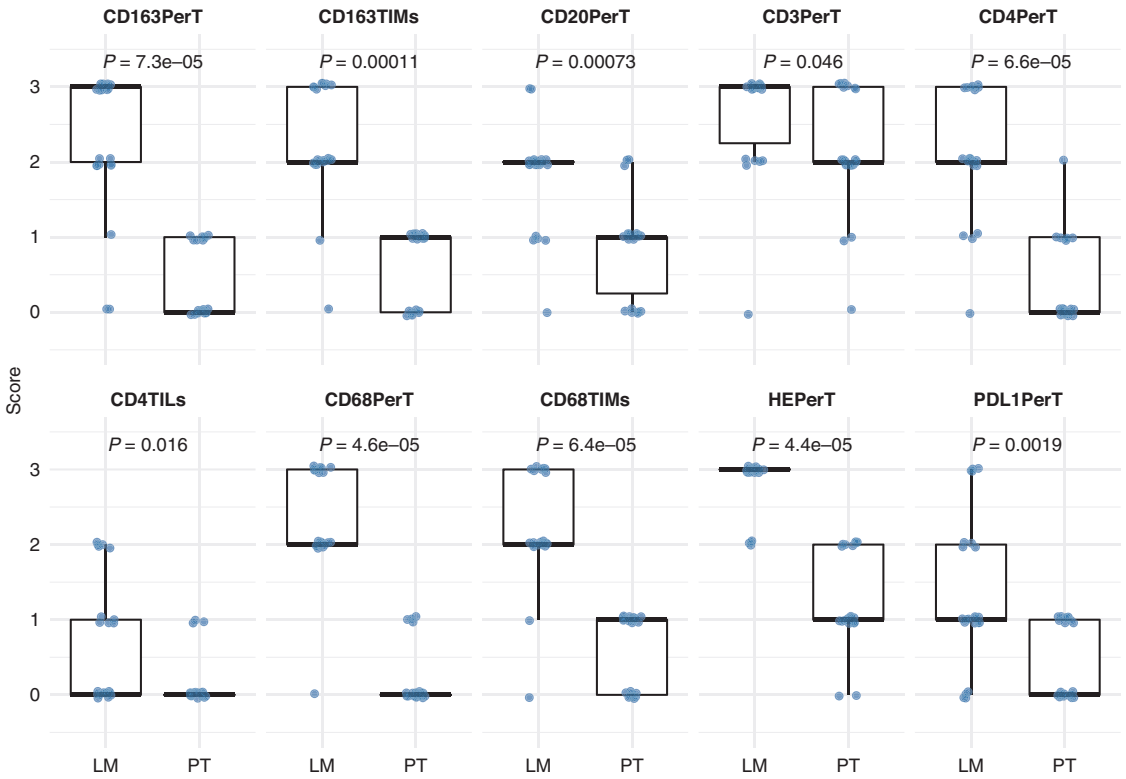

Fig. 1 Boxplots showing significant differences in immune staining scores between paired primary tumours (PT) and liver metastases (LM) of uveal melanoma. The immune parameter for which significant differences were noted is indicated on top of each graph.

in the metastases (Supplemental Table 1 and Fig. 3). In addition, peri-tumoral CD20+, PD-1+ lymphocytes were present in greater numbers in UMLM than in PUM in the total PUM-UMLM cohort (Supplemental Table 1, highlighted in bold). In addition, CD4+ and CD20+ TILs and CD68+ and CD163+TIMs were more conspicuous in UMLM than in PUM (Supplemental Table 1 and Fig. 4b). FoxP3 TILs appeared increased in PUM vs UMLM in the total PUM-UMLM cohort only (Supplemental Table 1). However, in general, TILs (HES, CD3, CD4, FoxP3, CD8, CD20 and PD-1) were scant (<5%) in both primary and metastatic tumours (Figs. 1 and 2). CD8+ and FoxP3+ peri-tumoral infiltrates and HES-stained, CD3+, FoxP3+, CD8+, and PD-1 TILs were of comparable density (not significantly different) in both PUM and UMLM. The results examining the distribution and density of ICI in paired PUM-UMLM vs total (containing unpaired and paired) PUM-UMLM were thus concordant for 17/20 ICI variables. As mentioned above, the only discordance between the latter groups related to scoring differences in total PUM-UMLM: FoxP3 TILs were more frequent in PUM than UMLM ($P = 0.028$), and CD20TILs ($P = 0.0074$) and PD-1 perT infiltrates ($P = 0.004$) had greater density in UMLM than PUM. In contrast, no differences were observed in the paired groups.

Immune checkpoint analysis in PUM and UMLM. PD-1 infiltrates analysed with the scoring system outlined above for TILs and perTumoral infiltrates revealed that PD-1 TILs had mean scores of 0.5 or <5% in PUM and 0.6 or <5% in UMLM, respectively, whereas peri-tumoral PD-1 infiltrates had mean scores of 0.7 or <5% of the PUM peri-tumoral area and 1.3 or slightly >5% of the UMLM peri-tumoral area, respectively (Supplemental Table 2).

PD-L1 analysis in PUM revealed a mean intra-tumoral expression of 9.4% (Supplemental Fig. 1) whereas in UMLM the mean expression was 3.2%. PD-L1 perTumoral (stromal) mean expression in PUM was 0.5%, while this mean expression was 9.2% in UMLM (Supplemental Fig. 2) (Supplemental Table 2).

Association of ICI and immune checkpoints with other variables in UMLM. The associations of the ten markers (HES, CD3, CD4, CD8, CD20, CD68, CD163, FOXP3, PD-1 and PD-L1) in the 2 distinct locations (perTumoral and intra-tumoral (TILs)) and the variables in Table 2 were analysed using the Kruskal–Wallis method. An important association of peri-tumoral CD3+ ($P = 0.047$), CD68+ ($P = 0.0038$) and CD163+ ($P = 0.0037$) infiltrates with the desmoplastic HGP was observed (Fig. 5 and Supplemental Table 3). Examination of UMLMs with 80–100% desmoplastic HGP has shown almost all with infiltrates achieving a score of 3 (infiltrates involving >50% of the perTumoral–stromal rim) for the latter variables. Other than a negative correlation with latter ICI, the replacement HGP showed no significant association with any immune parameter. No evidence of a link between T-cell or other immune cell infiltration in UMLM and either BAP1 mutation or monosomy 3 was demonstrated.

Analysis of survival in PUM. The median OS and MSOS in this series were respectively 49.7 (34.7–NA) and 26.2 (16.3–82.5) months. OS and MSOS were analysed with reference to the immune scores using Kaplan–Meier and Cox proportional hazards regression univariate and multivariate analysis. Important findings included the lack of any predictive value of TILs as assessed by HES and the following immunomarkers: CD3, CD4, CD8, CD20, FoxP3, PD-1, PD-L1 (tumour cell expression only). Although not significant on follow-up without limit, both CD68+ and CD163+ TIMs in PUM nonetheless had a favourable effect on prognosis at 10 years (Supplemental Figs. 3 and 4).

Analysis of survival in UMLM. OS and MSOS were analysed with reference to the immune scores and HGPs in UMLM using Kaplan–Meier and Cox proportional hazards regression univariate and multivariate analysis. In the multivariate Cox analysis, the HGP classification was added to the model for those immune scores that were significant on univariate analysis. Univariate analysis for OS revealed that age ($P = 0.001$), PUM diameter ($P = 0.016$), HGP

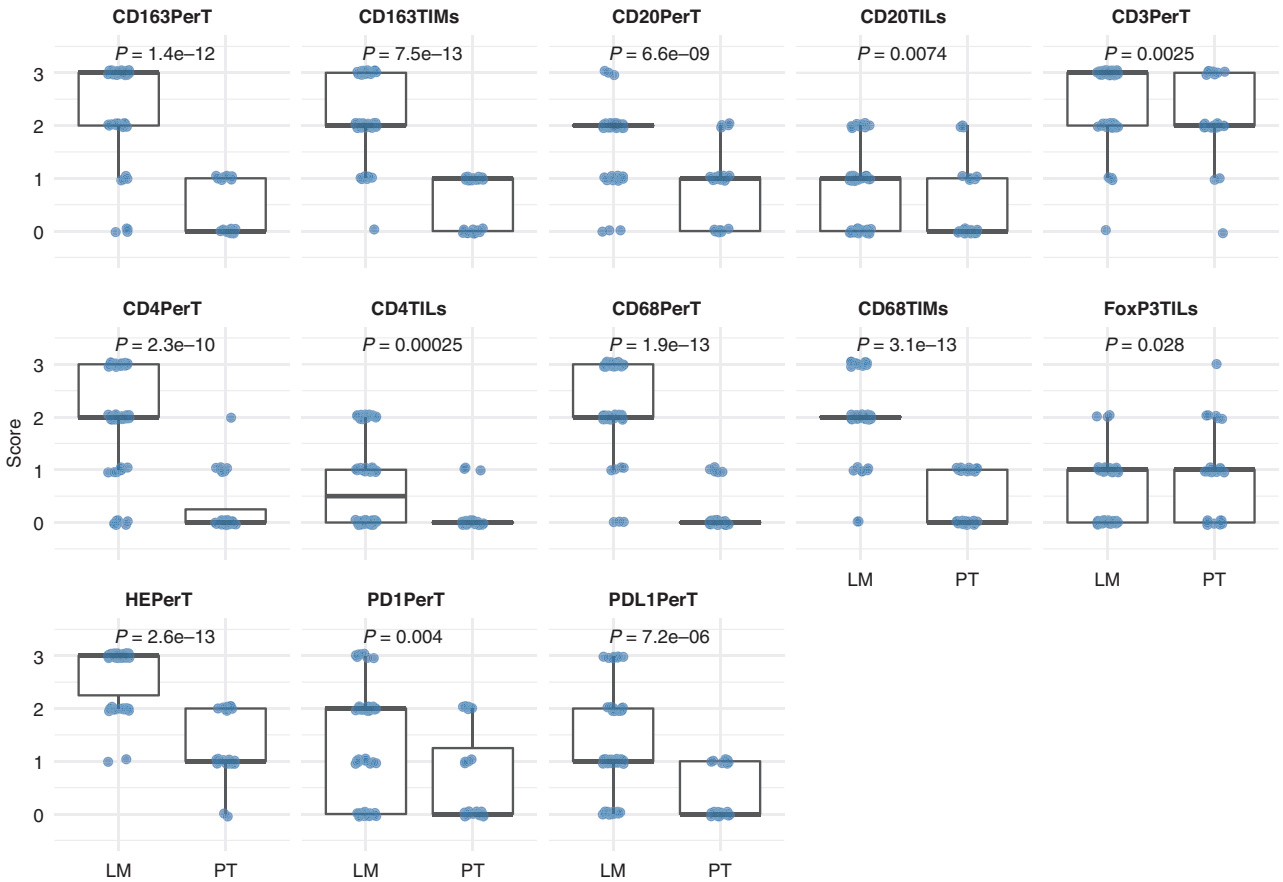

Fig. 2 Boxplots showing significant differences in immune staining scores between all primary tumours (PT) and liver metastases (LM) of uveal melanoma. The immune parameter for which significant differences were noted is indicated at top of each graph.

($P = 0.029$), aCGH (M3/8 G) ($P = 0.009$), CD20 perT ($P = 0.005$) (Supplemental Fig. 5), CD68 TIMs ($P = 0.001$) (Fig. 6a), CD68 perT ($P = 0.048$) (Supplemental Fig. 6) and CD163 perT ($P = 0.002$) (Supplemental Fig. 7), were significant (Supplemental Table 4). However, only age ($P = 0.001$), aCGH (M3/8 G) ($P = 0.018$), HGP ($P = 0.039$), and CD68 TIMs ($P = 0.002$) remained significant on multivariate analysis (Supplemental Table 5). With univariate analysis for MSOS, in addition to HGP, CD20 perT ($p = 0.002$) (Supplemental Fig. 8), CD68 TIMs ($P = 0.0001$) (Fig. 6b), and CD163 perT ($P = 0.014$) (Supplemental Fig. 9) were significant (Supplemental Table 6). On multivariate analysis, only HGP ($P = 0.030$), and CD68 TIMs ($p = 0.002$) remained significant (Supplemental Table 7). UMLM patients with high intra-tumoral CD68 macrophagic infiltration had a highly significant ($P < 0.0001$) improved MSOS in a dose-response fashion: patients with >50% CD68 infiltration has a median MSOS of more than 100 months; 5–50% CD68 infiltration a median MSOS > 75 months; <5% CD68 infiltration a median MSOS < 50 months; and the absence of intratumoral CD68 infiltrates a median OS < 25 months.

DISCUSSION

We report herein a comprehensive analysis of immune cell infiltrates, PD-1, and PD-L1 by conventional microscopy and immunohistochemistry in patients with uveal melanoma liver metastases. Our study cohort is unique since it is comprised entirely of surgically resected histopathologically documented UMLM derived from a large cohort of living patients. Direct comparison of our results with previous studies of UMLM is difficult because of the limitations of those studies owing to small sample size, the inclusion of inadequate small core (or fine-needle aspiration) biopsies, the inclusion of autopsy material, and finally differences in study design, methodologies, and techniques. In the present study, patients with liver biopsies and autopsy material only were excluded. The examination of fully resected UMLM in this work has permitted the comprehensive HES and IHC examination of the entire metastasis and surrounding perTumoral stroma in a 2-dimensional cross-sectional area in every case. A potential limitation of this study is that only a single tissue section, rather than multiple sections, from each metastasis was studied with each immune cell marker. Thus some heterogeneity in metastases and sampling differences could potentially lead to some inconsistencies in our results. This study is also unique since histopathological growth patterns were recorded for the first time in a large series of fully resected UM liver metastases and correlated with ICI and immune checkpoints in UMLM. HGPs in UMLM already reported by us are a major advance in the understanding of the biology and prognosis of UMLMs [7, 8]. Paired PUM from one-third of the patients including some additional PUM ($N = 28$) were also examined. The results of IHC from PUM and UMLM were compared and correlated not only with conventional clinical and histopathological prognostic factors but also with genomic risk groups, BAP1 mutational status, HGPs of UMLM, and both OS and MSOS.

Other strengths of the current study also stem from the detailed analysis of each ICI subset and checkpoint in both the intratumoral ("tumour infiltrating lymphocytes/macrophages" (TILs/TIMs)) and peri-tumoral/stromal compartments with respect to percentage cellular density in both the primary and metastatic tumours. Despite a previous report by Qin et al. [40], ICI expansion during UM metastatic evolution has not been sufficiently studied. We have shown that the expansion of ICI is strikingly predominant in the perTumoral area and comprised of both lymphocytes and

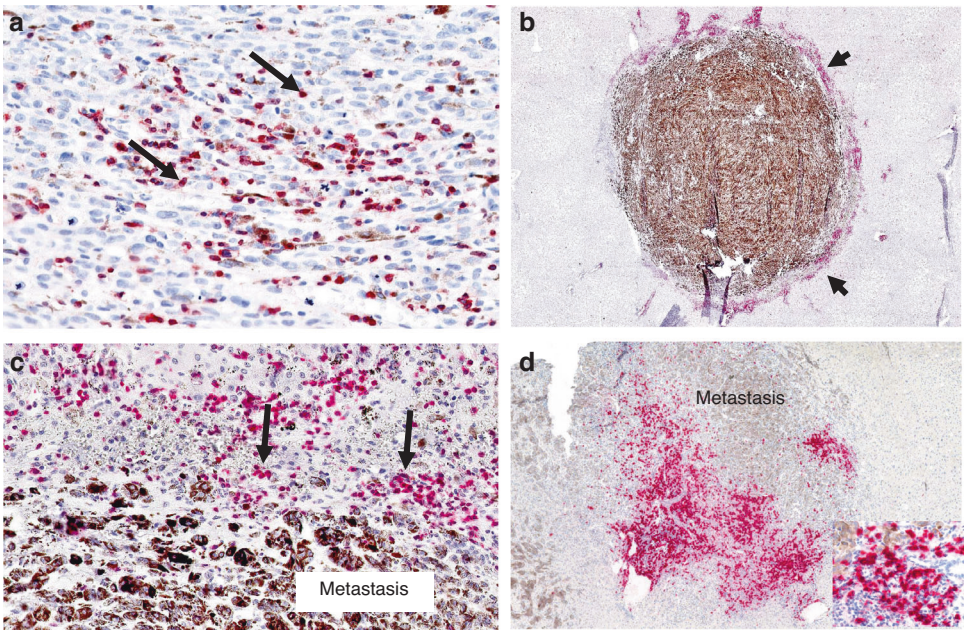

Fig. 3 Immunohistochemistry showing expression of lymphocyte markers in primary uveal melanoma and uveal melanoma liver metastases. a Primary uveal melanoma. Moderate CD3 TILs (arrows) expression (red chromogen) (score = 2; 5–50%). **b** Uveal melanoma liver metastasis. Intense peri-tumoral CD3 infiltrate (arrowheads) (red chromogen) (score = 3; >50%) surrounds heavily pigmented metastasis. **c** Higher magnification of (**b**). Arrows highlight CD3+ peri-tumoral lymphocytes. **d** Uveal melanoma liver metastasis. Prominent peri-tumoral CD20 infiltrates (red chromogen). Inset (right lower) shows CD20+ lymphocytes.

macrophages. Univariate and multivariate analysis revealed that intra-tumoral CD68+ infiltrates were strongly associated with increased OS and MSOS in UMLMs. In addition, increased CD68 +, CD163 +, CD20+ peri-tumoral (perT) infiltrates were associated with increased OS on univariate analysis. Further, CD3 +, CD68+ and CD163+ perT ICI are significantly linked to the desmoplastic HGP (Supplementary Table 2), which also connotes a favourable prognosis [7, 8, 30]. Our results provide evidence that the desmoplastic HGP has an "inflamed immune" phenotype, as suggested in the literature [36].

In this study, CD68+ and CD163+ infiltrates emerge as key participants in UMLM due to: (1) their increased numbers, both as tumour-infiltrating macrophages (TIMs) and perT macrophages and (2) their prognostic significance in UMLM (see above). The potential biological and prognostic influences of macrophages in UM have been investigated for more than 2 decades. CD68+ macrophagic infiltration was initially reported as an adverse prognostic factor in PUM [26, 28]. Although increased OS with both CD68+ and CD163+ TIMs was demonstrated at 10 years follow-up in the current study of 28 PUMs, no overall prognostic effect of these 2 markers was seen with longer-term follow-up.

Recently, greater attention has been placed on understanding ICIs in UMLMs, in order to develop effective immunotherapies at the metastatic stage. Initial studies mostly focused on TILs [39, 40] rather than macrophages. However, Krishna et al. [41] recently reported a higher frequency of macrophages than lymphocytes in ICI in 35 UMLM samples. Both CD68+ and CD163+ tumour-associated macrophages (TAMs) were observed in all UMLM analysed, mostly with "moderate" to "few" numbers of TAMs and mostly of "indeterminate" and "dendritic" cytomorphologies. At least three-quarters of macrophages within UMLM were of M2 subtype. Limitations of the latter study were that only 19 fully resected UMLM were examined and both needle biopsies and autopsy material were included. The study did not provide clear-cut distinction of intra-tumoral vs peri-tumoral spatial localisation of macrophages in all cases.

Tosi et al. [42] utilised multiplex immunofluorescence to characterise the immune cell landscape in 17 hepatic and 4 extra-hepatic metastases which was correlated with cytotoxic treatment response and survival. The density of individual infiltrating ICIs expressing CD3, CD4, CD8, FoxP3, CD20, CD56, CD68, CD163, neutrophil elastase, and granzyme B had no prognostic effect. Nonetheless, these authors called attention to the functional importance and clinical relevance of macrophage spatial localisation and potential intra/perTumoral ratios of ICIs. In contrast, Johansson et al. [43] demonstrated increased overall survival associated with CD68+ (but not CD163 +) TIMs and CD8+ TILs in 2 cohorts of 28 and 14 uveal melanoma liver metastases treated with hyperThermic isolated hepatic perfusion with melphalan. Limitations of the latter studies are small cohort size and biopsy sampling. Recent transcriptomic analyses of ICI including TAMs [44, 45] have yielded pertinent information about gene signatures associated with different cell types. NanoString analysis of pre- and post-immunotherapy samples of 27 PUM and 31 UMLM from 47 patients [44] demonstrated upregulation of an interferon-γ signature in pre-treatment tumours of responders, versus upregulation of a panel of pro-inflammatory cytokines and molecules in non-responders. However, the latter studies lack specificity with respect to the spatial localisation of and the type of ICI investigated.

The interpretation of any results related to macrophages expressing CD68 and CD163 and their relationships to M1 and M2 phenotypes in UMLM, or in any type of cancer, must consider the striking plasticity of these subsets as a function of spatial localisation and microenvironmental factors [46]. In particular, while CD68 (KP-1) expression has been associated with M1 (pro-inflammatory) macrophages, it is also expressed in other macrophages and myeloid cells [47, 48]. Our findings are in line with other studies demonstrating that the KP-1/CD68 phenotype, while not specific for M1, correlates with a pro-inflammatory phenotype and an important favourable prognostic effect [47, 48]. On the other hand, since the M2 macrophage phenotype is reported to be immunosuppressive, pro-tumorigenic, and predominant in many cancers, therapeutic strategies to diminish M2 macrophages, or "M1 polarisation", are considered desirable in the management of patients with cancer. However, CD163 is specific

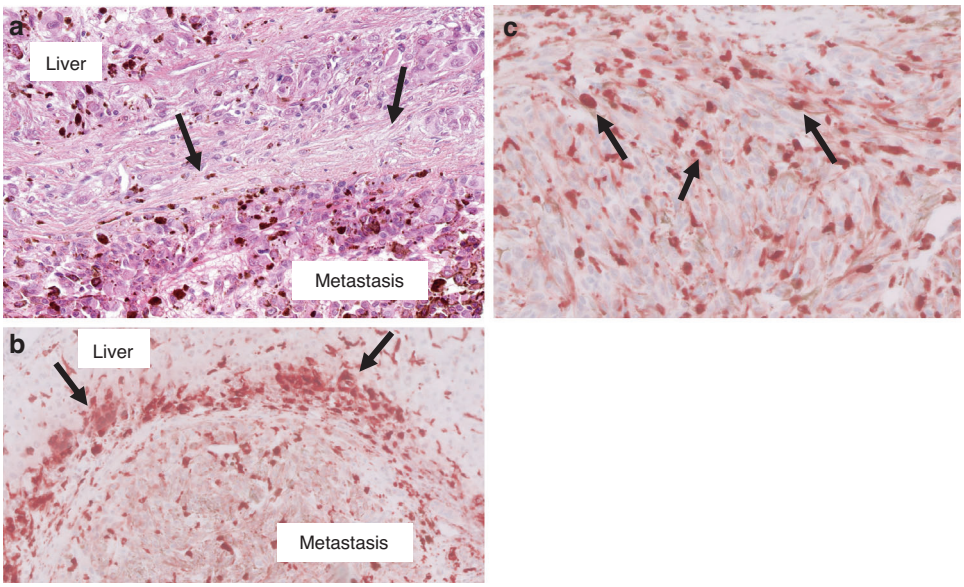

Fig. 4 Immunohistochemistry showing expression of macrophage markers in uveal melanoma liver metastases. a Uveal melanoma liver metastasis with desmoplastic histopathological growth pattern (HES stain). The metastasis (lower half of this image) is separated from the liver (upper part of the field) by a distinct thickened band of desmoplastic collagen (arrows). **b** Peri-tumoral band-like CD163 infiltrate (arrows) (reddish-brown chromogen) associated with the desmoplastic annulus, as seen in (**a**). **c** Uveal melanoma liver metastasis. CD68+ tumour-infiltrating macrophages (arrows) present within the metastasis (score =3; >50% of tumour area contains these TIMs).

to only a subset of M2 macrophages [48]. In order to explain the apparent comparable expression of CD68 and CD163 in UMLM, one must consider that "co-expression" or overlapping activation states of these 2 markers is occurring, as in other cancers, and that the overall effect is "pro-inflammatory" or prognostically favourable [48]. The latter explanation also appears applicable to the apparent favourable prognostic effect of both CD68+ and CD163+ perT infiltrates in PUM. In any case, our results highlight the relevance of studying in much greater detail CD68+ and CD163+ TIMs and perT tumoral macrophages in the microenvironment of UMLMs. For example, if confirmed by additional study, routine IHC could assist in estimating the OS and MSOS associated with intra-tumoral CD68+ macrophages, the strongest favourable prognostic factor among ICI in liver UMLM.

With reference to lymphocytic infiltrates, our observations are contrary to what we observed with macrophages, almost point-by-point: these infiltrates are relatively scant, with the exception of perTumoral lymphocytes (HES, CD3) in UMLM; TILs have no prognostic value (see below); and no expansion of TILs or CD8 cells is observed during metastatic evolution based on examination of paired PUM and UMLM samples. In fact, CD4, CD8, CD20, PD-1, and FoxP3 TILs were sparse in both PUM and UMLM. In addition, we have found no evidence that increased numbers of TILs in UMLM (or PUM) correlate with BAP1 mutation or monosomy 3 [18, 27].

Importantly, we have shown that the 2 most frequently studied lymphocytic parameters: HES-stained TILs and CD8+ TILs had no significant prognostic value in PUM or UMLM. Other TILs as studied by IHC analysis—CD3, CD4, CD20, FoxP3, and PD-1—also showed no effect on survival in PUM or UMLM. However, an unexpected finding was increased OS and MSOS associated with increased perTumoral CD20+ lymphocytes in UMLM ($P = 0.0031$).

The prognostic effect of B cell infiltrates in UMLM has received almost no attention. However, perTumoral CD20+ lymphocytes could have biological relevance, as a possible marker of Tertiary Lymphoid Structures (TLS) [49]. TLS have already been described as boosting immunotherapeutic response and survival in cutaneous melanoma [50] but have not yet been systematically studied in UM [51]. Sautes et al. described weak expression of the TLS signature in tumours occurring in immunologically privileged sites, such as the brain (glioblastoma and lower-grade glioma) and the eye (uveal melanoma), although tumours occurring in the testis (testicular germ cell tumours) exhibit a remarkably high expression of the TLS signature [52]. However, if TLS in UM behave as TLS in glioblastoma, one may hypothesise that TLS could enhance priming of tumour antigen-targeted T cells and sensitise tumours for immunotherapy [53]. Moreover, as far as metastases are concerned, Lee et al. demonstrated that the organs seeded by metastases may influence the densities of TLSs [54].

Rothermel et al. [39], conducted one of the first IHC studies of UMLM comparing ICI in 16 UM liver metastases versus the infiltrates in 35 liver metastases from cutaneous melanoma (MCM). These authors reported predominant CD4+ infiltrates in UMLM in contrast to CD8+ predominant infiltrates in MCM [39]. However, Krishna et al. reported few CD4 + T cells within UMLMs, although "numerous perivascular" CD4 infiltrates were recorded. In contrast, CD8+ cytotoxic/killer T cells were described as "predominantly encircling" the entire metastatic deposit. These authors suggested that CD4 + T cells and, in particular, CD8+ cells were not functional, since they were excluded from the tumour mass [41]. Qin et al. in comparing MCM and UMLM, found no differences in CD8 + TILs [40]. However, the TILs in UMLM were considered less functional than in MCM because of a lower rate of successful TIL expansion. Despite sparse numbers of TILs and/or CD8+TILs in UMLMs, some authors have nonetheless still described them as having prognostic value as mentioned above [42, 43].

Although PUM has been considered an immunosuppressive (immune privileged) environment and TILs and TIMs indicative of poor prognosis, critical examination of the literature discloses the lack of sufficient objective information concerning TILs in PUM. For example, TILs in PUM have been reported to have positive, negative, or no effect on prognosis [16, 18–22]. In fact, striking differences among the studies thus far reported including the lack of standardisation of techniques and methodologies, bias in the selection of cases, and insufficient number of cases and follow-up preclude any definitive conclusions about TILs in PUM. Larger multi-institutional studies with standardised methodology are needed.

With reference of immune checkpoints, it is well-established that PD-L1 appears to have little predictive value in UM and few patients appear to respond to anti-PD-1 therapy [49, 50]. In our analysis of PD-1/PD-L1 immune checkpoint expression in UMLMs

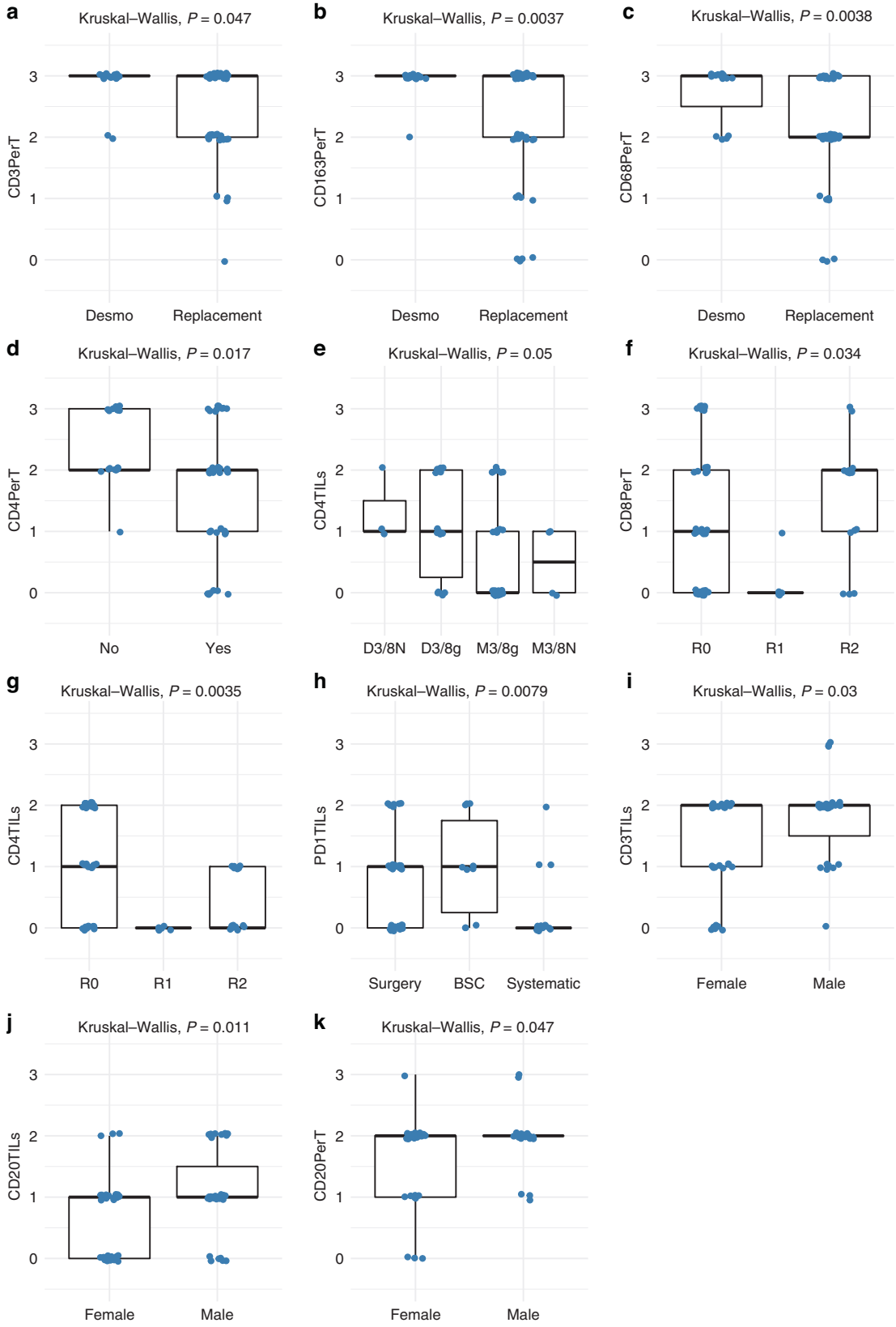

Fig. 5 Boxplots showing significant differences for immune cell infiltrates in uveal melanoma liver metastases analysed for various prognostic factors. **a**–**c** Uveal melanoma liver metastases stratified according to predominant desmoplastic or replacement histopathological growth pattern, **d** BAP1 loss, **e** aCGH risk group, **f**, **g** resection margins, **h** treatment, and **i**–**k** and gender. The immune parameters for which significant differences were noted are indicated along the *Y*-axis (Kruskal–Wallis test).

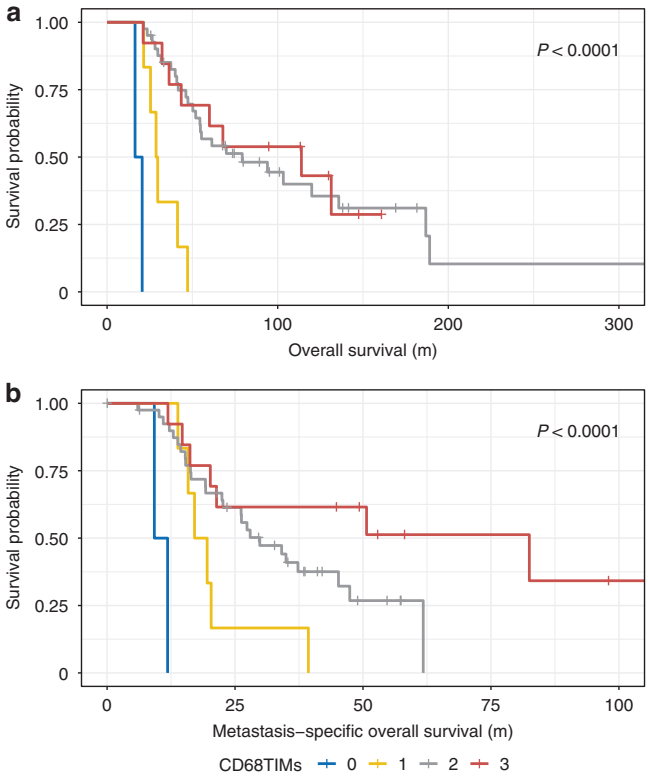

Fig. 6 Uveal melanoma liver metastases and CD68 tumour-infiltrating macrophages (TIMs). Kaplan–Meier plots. **a** Overall survival is increased as function of increasing percentage of CD68 TIMs. **b** Metastasis-specific overall survival is increased as a function of increasing percentage of CD68 TIMs.

and paired PUMs, PD-1 TILs were scant in both PUM and UMLM (<5%), and not significantly different, as expected since HES TILs and CD8+ TILs were also scant. PD-L1 also showed relatively low expression in both PUM (9.4%) and UMLM (3.2%), which is consistent with data in the literature [55] showing far less expression in UM as compared to cutaneous melanoma (35%). which could explain why the immune response is so limited in uveal melanoma and why other factors may be involved [56, 57].

In conclusion, our findings in depicting the immune landscape of UMLM show that ICI are mainly peri-tumoral and have greater density than those in PUM. On the other hand, TILs are scant and appear to have no prognostic value in either UMLM or PUM. In contrast, TIMs are numerous, and CD68+ TIMs constitute the sole ICI with independent prognostic effect in UMLM with respect to both OS and MSOS. It is of interest that CD68 TIMs and HGPs were the only factors remaining significant on multivariate analysis for MSOS. However, peri-tumoral CD68+ and CD163+ macrophagic and CD20+ lymphocytic perTumoral infiltrates also have favourable prognostic value.

Our results suggest the immediate importance of studying comprehensively macrophage subsets and CD20 infiltrates with respect to their particular tumoral and perTumoral localisation in the microenvironment of UMLMs and in the replacement and desmoplastic HGPs. Our study sheds light on the potential utility of 2 macrophage markers CD68 and CD163, as being particularly relevant to the biology, prognosis, and possibly therapy of patients with UM liver metastases.

DATA AVAILABILITY

All data are available upon request in writing from the corresponding author Raymond Barnhill.

REFERENCES

1. Radivoyevitch T, Zabor EC, Singh AD. Uveal melanoma: long-term survival. PLoS ONE. 2021;16:e0250939.
2. Zabor EC, Radivoyevitch T, Singh AD, Kilic E, de Klein JEMM, Kalirai H, et al. Conditional survival in uveal melanoma. Ophthalmol Retin. 2021;5:536–42.
3. Xu Y, Lou L, Wang Y, Miao Q, Jin K, Chen M, et al. Epidemiological study of uveal melanoma from US surveillance, epidemiology, and end results program (2010-2015). J Ophthalmol. 2020;2020:3614039.
4. Kaliki S, Shields CL. Uveal melanoma: relatively rare but deadly cancer. Eye Lond Engl. 2017;31:241–57.
5. Robertson AG, Shih J, Yau C, Gibb EA, Oba J, Mungall KL, et al. Integrative analysis identifies four molecular and clinical subsets in uveal melanoma. Cancer Cell. 2017;32:204–20.e15.
6. Cassoux N, Rodrigues MJ, Plancher C, Asselain B, Levy-Gabriel C, Rouic LL-L, et al. Genome-wide profiling is a clinically relevant and affordable prognostic test in posterior uveal melanoma. Br J Ophthalmol. 2014;98:769–74.
7. Barnhill R, Vermeulen P, Daelemans S, van Dam P-J, Roman-Roman S, Servois V, et al. Replacement and desmoplastic histopathological growth patterns: A pilot study of prediction of outcome in patients with uveal melanoma liver metastases. J Pathol Clin Res. 2018;4:227–40.
8. Barnhill R, van Laere S, Vermeulen P, Roman-Roman S, Gardrat S, Alsafadi S, et al. L1CAM and laminin vascular network: Association with the high-risk replacement histopathologic growth pattern in uveal melanoma liver metastases. Lab Invest. 2022; https://doi.org/10.1038/s41374-022-00803-w.
9. Orloff M. Clinical trials in metastatic uveal melanoma: immunotherapy. Ocul Oncol Pathol. 2021;7:168–76.
10. Ny L, Jespersen H, Karlsson J, Alsén S, Filges S, All-Eriksson C, et al. The PEMDAC phase 2 study of pembrolizumab and entinostat in patients with metastatic uveal melanoma. Nat Commun. 2021;12:5155.
11. Minor DR, Kim KB, Tong RT, Wu MC, Kashani-Sabet M, Orloff M, et al. A pilot study of hepatic irradiation with yttrium-90 microspheres followed by immunotherapy with ipiliumlmab and nivolumab for metastatic uveal melanoma. Cancer Biother Radiopharm. 2022;37:11–16.
12. Pelster MS, Gruschkus SK, Bassett R, Gombos DS, Shephard M, Posada L, et al. Nivolumab and IpiliUMLMab in metastatic uveal melanoma: results from a single-arm phase II study. J Clin Oncol J Am Soc Clin Oncol. 2021;39:599–607.
13. Piulats JM, Espinosa E, de la Cruz Merino L, Varela M, Alonso Carrión L, Martín-Algarra S, et al. Nivolumab plus IpiliUMLMab for treatment-naïve metastatic uveal melanoma: an open-label, multicenter, phase II trial by the Spanish Multidisciplinary Melanoma Group (GEM-1402). J Clin Oncol J Am Soc Clin Oncol. 2021;39:586–98.
14. Middleton MR, McAlpine C, Woodcock VK, Corrie P, Infante JR, Steven NM, et al. Tebentafusp, a TCR/Anti-CD3 bispecific fusion protein targeting gp100, potently activated antitumor immune responses in patients with metastatic melanoma. Clin Cancer Res J Am Assoc Cancer Res. 2020;26:5869–78.
15. Nathan P, Hassel JC, Rutkowski P, Baurain JF, Butler MO, Schlaak M, et al. Overall survival benefit with tebentafusp in metastatic uveal melanoma. N. Engl J Med. 2021;385:1196–206. https://doi.org/10.1056/NEJMoa2103485.
16. Lagouros E, Salomao D, Thorland E, Hodge DO, Vile R, Pulido JS. Infiltrative T regulatory cells in enucleated uveal melanomas. Trans Am Ophthalmol Soc. 2009;107:223–8.
17. Whelchel JC, Farah SE, McLean IW, Burnier MN. Immunohistochemistry of infiltrating lymphocytes in uveal malignant melanoma. Invest Ophthalmol Vis Sci. 1993;34:2603–6.
18. Bronkhorst IHG, Vu THK, Jordanova ES, Luyten GPM, van der Burg SH, Jager MJ. Different subsets of tumor-infiltrating lymphocytes correlate with macrophage influx and monosomy 3 in uveal melanoma. Invest Ophthalmol Vis Sci. 2012;53:5370–8.
19. Bronkhorst IHG, Jager MJ. Inflammation in uveal melanoma. Eye Lond Engl. 2013;27:217–23.
20. Göllnitz R, Lommatzsch PK. [Prognostic significance of lymphocytic infiltration in malignant melanoma of the choroid]. Klin Monatsbl Augenheilkd. 1988;192:660–5.
21. de la Cruz PO, Specht CS, McLean IW. Lymphocytic infiltration in uveal malignant melanoma. Cancer. 1990;65:112–5.
22. Lang JR. Lost to follow-up. Arch Ophthalmol. 1977;95:1082.
23. Mougiakakos D, Johansson CC, Trocme E, All-Ericsson C, Economou MA, Larsson O, et al. Intratumoral forkhead box P3-positive regulatory T cells predict poor survival in cyclooxygenase-2-positive uveal melanoma. Cancer. 2010;116:2224–33.
24. van Essen TH, van Pelt SI, Versluis M, Bronkhorst IHG, van Duinen SG, Marinkovic M, et al. Prognostic parameters in uveal melanoma and their association with BAP1 expression. Br J Ophthalmol. 2014;98:1738–43.
25. Maat W, Ly LV, Jordanova ES, de Wolff-Rouendaal D, Schalij-Delfos NE, Jager MJ. Monosomy of chromosome 3 and an inflammatory phenotype occur together in uveal melanoma. Invest Ophthalmol Vis Sci. 2008;49:505–10.

26. Bronkhorst IHG, Ly LV, Jordanova ES, Vrolijk J, Versluis M, Luyten GPM, et al. Detection of M2-macrophages in uveal melanoma and relation with survival. Invest Ophthalmol Vis Sci. 2011;52:643–50.
27. Gezgin G, Dogrusöz M, van Essen TH, Kroes WGM, Luyten GPM, van der Velden PA, et al. Genetic evolution of uveal melanoma guides the development of an inflammatory microenvironment. Cancer Immunol Immunother. 2017;66:903–12.
28. Mäkitie T, Summanen P, Tarkkanen A, Kivelä T. Tumor-infiltrating macrophages (CD68(+) cells) and prognosis in malignant uveal melanoma. Invest Ophthalmol Vis Sci. 2001;42:1414–21.
29. Mantovani A, Sozzani S, Locati M, Allavena P, Sica A. Macrophage polarization: tumor-associated macrophages as a paradigm for polarized M2 mononuclear phagocytes. Trends Immunol. 2002;23:549–55.
30. Barnhill R, van Dam P-J, Vermeulen P, Champenois G, Nicolas A, Rawson RV, et al. Replacement and desmoplastic histopathological growth patterns in cutaneous melanoma liver metastases: frequency, characteristics, and robust prognostic value. J Pathol Clin Res. 2020;6:195–206.
31. van Dam P-J, van der Stok EP, Teuwen L-A, Van den Eynden GG, Illemann M, Frentzas S, et al. International consensus guidelines for scoring the histopathological growth patterns of liver metastasis. Br J Cancer. 2017;117:1427–41.
32. Latacz E, Caspani E, Barnhill R, Lugassy C, Verhoef C, Grünhagen D, et al. Pathological features of vessel co-option versus sprouting angiogenesis. Angiogenesis. 2020;23:43–54.
33. Barnhill RL, Ye M, Batistella A, Stern M-H, Roman-Roman S, Dendale R, et al. The biological and prognostic significance of angiotropism in uveal melanoma. Lab Investig J Tech Methods Pathol. 2017; https://doi.org/10.1038/labinvest.2017.16.
34. McLean IW, Foster WD, Zimmerman LE, Gamel JW. Modifications of Callender's classification of uveal melanoma at the Armed Forces Institute of Pathology. Am J Ophthalmol. 2018;195:lvi–lx.
35. McLean IW, Foster WD, Zimmerman LE, Gamel JW. Modifications of Callender's classification of uveal melanoma at the Armed Forces Institute of Pathology. Am J Ophthalmol. 1983;96:502–9.
36. Latacz E, Höppener D, Bohlok A, Leduc S, Tabariès S, Fernández Moro C, et al. Histopathological growth patterns of liver metastasis: updated consensus guidelines for pattern scoring, perspectives and recent mechanistic insights. Br J Cancer. 2022; https://doi.org/10.1038/s41416-022-01859-7.
37. Ramtohul T, Ait Rais K, Gardrat S, Barnhill R, Román-Román S, Cassoux N, et al. Prognostic implications of MRI melanin quantification and cytogenetic abnormalities in liver metastases of uveal melanoma. Cancers. 2021;13:2728.
38. Viros A, Fridlyand J, Bauer J, Lasithiotakis K, Garbe C, Pinkel D, et al. Improving melanoma classification by integrating genetic and morphologic features. PLoS Med. 2008;5:e120.
39. Rothermel LD, Sabesan AC, Stephens DJ, Chandran SS, Paria BC, Srivastava AK, et al. Identification of an immunogenic subset of metastatic uveal melanoma. Clin Cancer Res J Am Assoc Cancer Res. 2016;22:2237–49.
40. Qin Y, Petaccia de Macedo M, Reuben A, Forget M-A, Haymaker C, Bernatchez C, et al. Parallel profiling of immune infiltrate subsets in uveal melanoma versus cutaneous melanoma unveils similarities and differences: a pilot study. Oncoimmunology. 2017;6:e1321187.
41. Krishna Y, McCarthy C, Kalirai H, Coupland SE. Inflammatory cell infiltrates in advanced metastatic uveal melanoma. Hum Pathol. 2017;66:159–66.
42. Tosi A, Cappellesso R, Dei Tos AP, Rossi V, Aliberti C, Pigozzo J, et al. The immune cell landscape of metastatic uveal melanoma correlates with overall survival. J Exp Clin Cancer Res CR. 2021;40:154.
43. Johansson J, Siarov J, Kiffin R, Mölne J, Mattsson J, Naredi P, et al. Presence of tumor-infiltrating CD8+ T cells and macrophages correlates to longer overall survival in patients undergoing isolated hepatic perfusion for uveal melanoma liver metastasis. Oncoimmunology. 2020;9:1854519.
44. Qin Y, Bollin K, de Macedo MP, Carapeto F, Kim KB, Roszik J, et al. Immune profiling of uveal melanoma identifies a potential signature associated with response to immunotherapy. J Immunother Cancer. 2020;8:e000960.
45. Lv X, Ding M, Liu Y. Landscape of infiltrated immune cell characterization in uveal melanoma to improve immune checkpoint blockade therapy. Front Immunol 2022;13:848455.
46. Zhou H, Gan M, Jin X, Dai M, Wang Y, Lei Y, et al. miR-382 inhibits breast cancer progression and metastasis by affecting the M2 polarization of tumor-associated macrophages by targeting PGC-1α. Int J Oncol. 2022;61:126.
47. Honkanen TJ, Tikkanen A, Karihtala P, Mäkinen M, Väyrynen JP, Koivunen JP. Prognostic and predictive role of tumour-associated macrophages in HER2 positive breast cancer. Sci Rep. 2019;9:10961.
48. Gao J, Liang Y, Wang L. Shaping polarization of tumor-associated macrophages in cancer immunotherapy. Front Immunol. 2022;13:888713 https://doi.org/10.3389/fimmu.2022.888713.
49. Sautès-Fridman C, Petitprez F, Calderaro J, Fridman WH. Tertiary lymphoid structures in the era of cancer immunotherapy. Nat Rev Cancer. 2019;19:307–25.
50. Cabrita R, Lauss M, Sanna A, Donia M, Skaarup Larsen M, Mitra S, et al. Tertiary lymphoid structures improve immunotherapy and survival in melanoma. Nature. 2020;577:561–5.
51. Cipponi A, Mercier M, Seremet T, Baurain J-F, Théate I, van den Oord J, et al. Neogenesis of lymphoid structures and antibody responses occur in human melanoma metastases. Cancer Res. 2012;72:3997–4007.
52. Ricketts TD, Prieto-Dominguez N, Gowda PS, Ubil E. Mechanisms of macrophage plasticity in the tumor environment: manipulating activation state to improve outcomes. Front Immunol. 2021;12:642285.
53. van de Walle T, Vaccaro A, Ramachandran M, Pietilä I, Essand M, Dimberg A. Tertiary lymphoid structures in the central nervous system: implications for glioblastoma. Front Immunol. 2021;12:724739.
54. Lee M, Heo S-H, Song IH, Rajayi H, Park HS, Park IA, et al. Presence of tertiary lymphoid structures determines the level of tumor-infiltrating lymphocytes in primary breast cancer and metastasis. Mod Pathol J U S Can Acad Pathol Inc. 2019;32:70–80.
55. Kaunitz GJ, Cottrell TR, Lilo M, Muthappan V, Esandrio J, Berry S, et al. Melanoma subtypes demonstrate distinct PD-L1 expression profiles. Lab Investig J Tech Methods Pathol. 2017;97:1063–71.
56. Rodrigues M, Mobuchon L, Houy A, Fiévet A, Gardrat S, Barnhill RL, et al. Outlier response to anti-PD1 in uveal melanoma reveals germline MBD4 mutations in hypermutated tumors. Nat Commun. 2018;9:1866.
57. Saint-Ghislain M, Derrien A-C, Geoffrois L, Gastaud L, Lesimple T, Negrier S, et al. MBD4 deficiency is predictive of response to immune checkpoint inhibitors in metastatic uveal melanoma patients. Eur J Cancer. 2022;173:105–12.

AUTHOR CONTRIBUTIONS

RB confirms that he had full access to the data in the study and final responsibility for the decision to submit for publication. RB wrote the manuscript with the assistance of NT, SVL and LK. RB developed the methodology. RB collected and analysed data. SVL performed statistical analyses and analysed data. LL, GC and AN performed immunohistochemistry, scanned glass slides, and managed glass microslides. PM and SPN collected data. All the authors reviewed and approved the manuscript.

FUNDING

This project has received funding from the European Union's Horizon 2020 research and innovation programme under grant agreement no. 667787.

COMPETING INTERESTS

The authors declare no competing interests.

ETHICS APPROVAL AND CONSENT TO PARTICIPATE

The study was approved by the Ethics Committee, Institut Curie. All patients agreed to participate in the study based on informed consent. The study was performed in accordance with the Declaration of Helsinki.

CONSENT FOR PUBLICATION

Not applicable.

ADDITIONAL INFORMATION

Supplementary information The online version contains supplementary material available at https://doi.org/10.1038/s41416-023-02331-w.

Correspondence and requests for materials should be addressed to Raymond Barnhill.

Reprints and permission information is available at http://www.nature.com/reprints

Publisher's note Springer Nature remains neutral with regard to jurisdictional claims in published maps and institutional affiliations.